

The role of wetting layer states on the emission efficiency of InAs/InGaAs metamorphic quantum dot nanostructures

L Seravalli¹, G Trevisi¹, P Frigeri¹, S Franchi¹, M Geddo² and G Guizzetti²

¹ CNR-IMEM, Parco delle Scienze 37a, I-43100, Parma, Italy

² CNISM-Dipartimento di Fisica 'A Volta', Università degli Studi di Pavia, Via Bassi 6, I-27100, Pavia, Italy

E-mail: seravall@imem.cnr.it

Received 5 March 2009, in final form 22 April 2009

Published 17 June 2009

Online at stacks.iop.org/Nano/20/275703

Abstract

We report on a photoluminescence and photoreflectance study of metamorphic InAs/InGaAs quantum dot strain-engineered structures with and without additional InAlAs barriers intended to limit the carrier escape from the embedded quantum dots. From: (1) the substantial correspondence of the activation energies for thermal quenching of photoluminescence and the differences between wetting layer and quantum dot transition energies and (2) the unique capability of photoreflectance of assessing the confined nature of the escape states, we confidently identify the wetting layer states as the final ones of the process of carrier thermal escape from quantum dots, which is responsible for the photoluminescence quenching. Consistently, by studying structures with additional InAlAs barriers, we show that a significant reduction of the photoluminescence quenching can be obtained by the increase of the energy separation between wetting layers and quantum dot states that results from the insertion of enhanced barriers. These results provide useful indications on the light emission quenching in metamorphic quantum dot strain-engineered structures; such indications allow us to obtain light emission at room temperature in the 1.55 μm range and beyond by quantum dot nanostructures grown on GaAs substrates.

1. Introduction

Self-assembled quantum dots (QDs) are nanostructures whose properties can be engineered within wide limits [1, 2]. The availability of GaAs-based photonic devices with room temperature emission redshifted to 1.55 μm and beyond is of great interest for lightwave communications, optical interconnections, free-space optical communication and medical [3] applications.

Recently, the use of metamorphic QDs was shown to be an effective approach towards this goal [4–7]; in particular, in this type of structure it has been demonstrated that the redshift of emission can be obtained in structures consisting of InAs QDs embedded in InGaAs confining layers (CLs) deposited on GaAs substrates by reducing the strain exerted by CLs on QDs; this can be achieved: (i) by increasing the strain relaxation of the lower CL (LCL) by widening

its thickness [8–10] and/or (ii) by increasing the In mole fraction x of $\text{In}_x\text{Ga}_{1-x}\text{As}$; moreover, the increase of x directly concurs to the redshift by means of the reduction of the band discontinuities that confine carriers into QDs [8, 9]. Such an approach, based on metamorphic structures and called *Quantum Dot Strain Engineering* (QDSE), results in room temperature (RT) emission wavelengths as long as 1.44 μm [8, 9]. It has been shown that longer emission wavelengths can be hardly obtained at RT by means of QDSE, since the reduction of band discontinuities causes the increase of thermal escape of carriers out of QDs, which is the main process that quenches the RT emission efficiency η [11, 12]. However, when QDs are embedded in nm-thick InAlAs layers with an energy gap larger than that of InGaAs CLs, such additional barriers are effective in enhancing carrier confinement and, then, η [4, 13]. Also in simpler structures InAlAs barriers have been shown to increase the emission

efficiency [14–16]. The emission blueshift related to the enhancement of barriers can be compensated for by a larger strain relaxation of QDs that can be obtained by slightly larger LCL thicknesses [4, 13]. By properly engineering the structures, RT emission wavelengths as long as $1.59 \mu\text{m}$ [4] and beyond [17] have been obtained, which are among the longest obtained with GaAs substrates.

A further step in the quest for long-wavelength emission ($>1.6 \mu\text{m}$) could be done by a deeper understanding of the carrier escape process and, in particular, by the identification of the final states of thermal transitions. While a number of works studied thermal quenching of light emission in various QD structures [18–21], in quantum dot strain-engineered (QDSEd) ones it still remains unclear what are the RT escape channels for thermally activated carriers, whether: (i) InGaAs CL states, (ii) wetting layer (WL) levels, (iii) defect states or (iv) QD excited states. As a matter of fact only some preliminary indications on the relevant role of WL states as escape channels in QDSEd structures were reported up to now [11].

In the present work, we report on a combined study by photoluminescence (PL) and photoreflectance (PR) of QDSEd InAs/InGaAs nanostructures with and without InAlAs barriers; the work is aimed at confirming previous indications [11] on the effective escape channel and extending them to structures with enhanced barriers. This is done by the identification of the role of WL levels in the PL thermal quenching process, taking advantage of unique properties of the PR technique. In PR a periodic modulation ΔR of the reflectance R of the sample is produced by modulating the surface (built-in) electric field through electron–hole pairs photo-excited by a pump source (laser). By using a monochromatized probe light and phase-sensitive detection PR signals $\Delta R/R$ as low as 10^{-6} can be revealed [22]. The PR derivative nature [23, 24] (e.g. near interband critical points in bulk semiconductors, the line-shape behaviour is proportional to the third derivative of the dielectric function with respect to the photon energy) emphasizes even weak structures and suppresses undesired background effects. The richness of the derivative-like spectra allows us, by means of the lineshape analysis, to determine the critical-point energy with an uncertainty of a few millielectronvolts even at room temperature [23]. Moreover, among the peculiar properties of PR we recall the ability to reveal the nature of the different transitions (bulk, quantum confined, band-to-band, excitonic, etc) due to the lineshape dependence on the specific type of critical point [23, 24].

2. Experimental details

The structures, grown by molecular beam epitaxy (MBE) on semi-insulating (100) GaAs substrates, consist of: (i) a 100 nm thick GaAs buffer layer grown at 600°C , (ii) an $\text{In}_x\text{Ga}_{1-x}\text{As}$ metamorphic lower confining layer (LCL) of thickness t (20–1000 nm) grown at 490°C , (iii) 3 ML InAs QDs deposited by atomic layer MBE (ALMBE [25]) at 460°C , and (iv) a 20 nm thick $\text{In}_x\text{Ga}_{1-x}\text{As}$ upper confining layer (UCL) grown by ALMBE at 360°C . Indium compositions $x = 0.15, 0.28$ and 0.31 were chosen. In structures with additional barriers a 6 nm thick $\text{In}_{1-y}\text{Al}_y\text{As}$ lower barrier ($y = 0.80, 0.85$ and

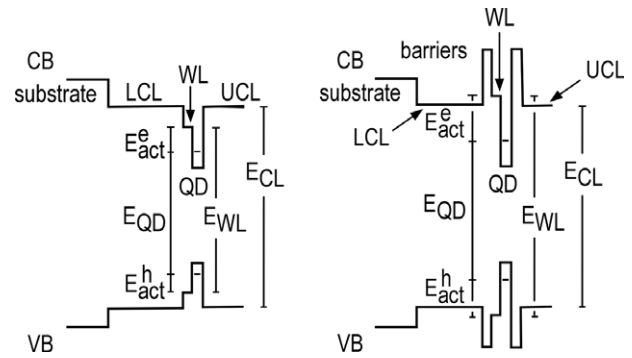


Figure 1. Profiles of conduction (CB) and valence (VB) bands along the growth direction of quantum dot strain-engineered structures without (left panel) and with (right panel) additional barriers; the energies of relevant transitions in confining layers (LCLs and UCLs, E_{CL}), wetting layer (WL, E_{WL}) and quantum dots (QDs, E_{QD}) are also shown. E_{act}^e and E_{act}^h are the activation energies for thermal escape of electrons and holes from QD states to WL ones. For the sake of simplicity, the strain-related splitting of valence bands is not shown. Not to scale.

0.90) and a 1 nm $\text{In}_x\text{Ga}_{1-x}\text{As}$ layer were deposited before QD growth, while after QDs a 6 nm $\text{In}_{1-y}\text{Al}_y\text{As}$ upper barrier was added [13]. Figure 1 schematically shows the conduction (CB) and valence (VB) band profiles along the growth direction of QDSEd structures without (left panel) and with (right panel) additional barriers.

PL was excited at 532 nm in the 10–300 K temperature range; the spectra were corrected for the spectral response of the set-up. PR measurements were performed at near-normal incidence in the 0.7–1.6 eV spectral window, with an energy step and spectral resolution of 1 meV. The modulation source was provided by a 20 mW 488 nm sapphire laser, mechanically chopped at a frequency of 220 Hz. Details on experimental apparatus and data analysis were reported elsewhere [26].

3. Results and discussion

Figure 2 shows typical PR spectra at RT for structures with $x = 0.15$ and $t = 60$ nm and with and without $y = 0.90$ additional barriers. In both cases at low energy the spectra are dominated by the heavy-hole (HH) and light-hole (LH) features³ of bandgap transitions ($E_{\text{CL}}^{\text{HH}}$ and $E_{\text{CL}}^{\text{LH}}$) split by residual strain in InGaAs metamorphic CLs [10]. The valence band splitting of CLs in different structures with the same x is independent of y and for $x = 0.15$ it is very close to the expected value in structures without enhanced barriers (56 meV) [10, 11]. This result ensures that the 6 nm thick InAlAs additional barriers have a negligible effect on the LCLs residual strain and then on the QD strain. At higher energies (~ 1.42 eV) figure 2 shows

³ Due to its derivative-like nature PR lineshape is characterized by the presence of one or more zero crossings; consequently, in contrast to what happens by using emission-like techniques such as PL and Raman shift, the transition energy usually does not coincide with the peak or valley position of the spectral feature (see [23] and [24]). Nevertheless it can be extracted from the best fit of the experimental spectra by using appropriate lineshape models (see, for example, figure in [10] and more details on the fitting procedure in [26]).

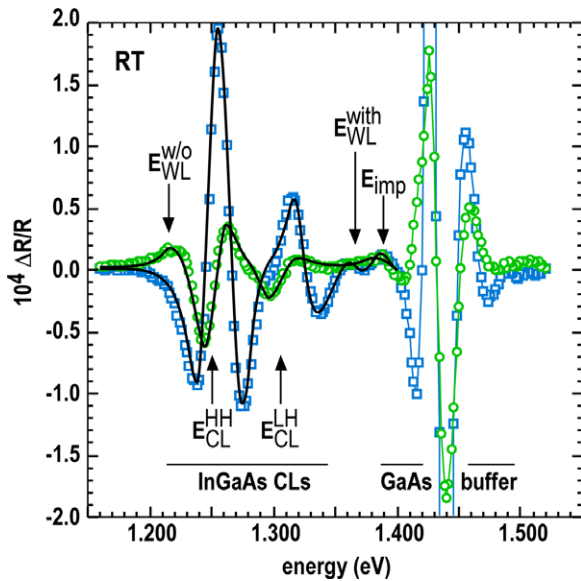


Figure 2. Typical RT PR spectra of $x = 0.15$ and $t = 60$ nm quantum dot strain-engineered structures with $y = 0.90$ additional barriers (squares) and without (circles). Arrows mark the energy position of the WL-related features ($E_{\text{WL}}^{\text{with}}$ and $E_{\text{WL}}^{\text{w/o}}$) in structures with and without additional barriers, of the split InGaAs bandgap transitions ($E_{\text{CL}}^{\text{HH}}$ and $E_{\text{CL}}^{\text{LH}}$) and of the impurity transition (E_{imp}) as obtained from the best fit of the experimental data (solid lines).

the PR features of the GaAs buffer bandgap including some lobes of Franz–Keldysh oscillations [24].

In the spectra of the structures without barriers the low energy feature labelled as $E_{\text{WL}}^{\text{w/o}}$ falls at an energy (~ 1.21 eV) very close to that previously observed in similar samples [11] and is assigned to the WL states since it has already been shown [11] that its QW-like PR feature [24, 27] must be related to the transition between electron and heavy-hole ground states in a two-dimensional system.

The experimental lineshapes (symbols) have been fitted (solid lines) by using the well-known Aspnes relation [23] with the characteristic exponent $n = 3$ to interpret the excitonic character of intersubband transitions in quantum confined systems [24, 27, 28] and $n = 2.5$ to reproduce bulk band-to-band transitions [23] due to three-dimensional M_0 critical points of the CLs' direct bandgap.

In structures with additional barriers the WL feature is blueshifted to higher energies ($E_{\text{WL}}^{\text{with}} \sim 1.36$ eV for $y = 0.90$, figure 2) in the spectral region below the GaAs bandgap. A similar behaviour was observed for $y = 0.80$, where $E_{\text{WL}}^{\text{with}}$ falls near 1.34 eV (not shown).

We note that our attribution of both $E_{\text{WL}}^{\text{w/o}}$ and $E_{\text{WL}}^{\text{with}}$ PR features to the WL states is supported by the following arguments.

- (i) In both cases, the best fit of the experimental lineshape according to the Aspnes relationship requires $n = 3$, which is typical of RT QW excitonic transitions [24, 27].
- (ii) Previous morphological studies on similar structures did not show the occurrence of either quantum wires or different ensembles of QDs other than those having the RT fundamental transitions at $E_{\text{QD}} = 0.950$ eV.

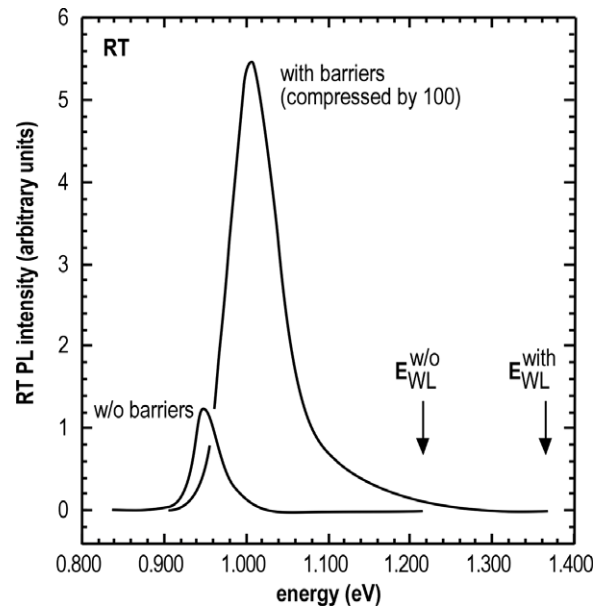


Figure 3. QD photoluminescence spectra at RT of $x = 0.15$ and $t = 60$ nm quantum dot strain-engineered structures with $y = 0.90$ additional barriers and without. The arrows mark the energy position of the WL-related features in the same structures with ($E_{\text{WL}}^{\text{with}}$) and without ($E_{\text{WL}}^{\text{w/o}}$) additional barriers as detected by PR (figure 2).

- (iii) Oscillator strength considerations rule out that the transitions we attribute to WL states may originate from QD excited states. As a matter of fact, the ground state transitions of QD nanostructures are usually very hard to detect at RT [28–30] (and even more for the excited states). In contrast, QW intersubband transitions maintain their excitonic character up to RT [27] and can be easily revealed by PR even in ultra-thin (monolayer-sized) structures [29, 31, 32].

Finally, the feature near 1.38 eV, denoted as E_{imp} in figure 2, can be attributed to shallow impurities [24] in the semi-insulating GaAs substrate or at the buffer–substrate interface. While this transition is not relevant for the present study, it turned out to be useful to take into account its contribution [23, 24] to the experimental lineshape to improve the best fits of the spectra.

In figure 3 we show the RT PL spectra of the same structures considered in figure 2 ($t = 60$ nm, $x = 0.15$ and, then, a QD-CL mismatch of 0.0697, with $\text{In}_{0.10}\text{Al}_{0.90}\text{As}$ barriers and without). The main features of the spectrum of the structure with barriers are: (i) the expected blueshift of emission (by ~ 50 meV) that takes place when additional barriers are used and (ii) the significant increase of the emission efficiency (by a factor of about 500), which will be discussed below.

In order to derive the activation energies of thermal quenching of PL, the temperature T dependence of the integrated PL intensity I was fitted by $I = I_0(1 + a \exp(-E_{\text{act}}/kT) + b \exp(-E'_{\text{act}}/kT))^{-1}$, where two thermally activated quenching processes are considered. The process with the larger activation energy E_{act} has been interpreted as

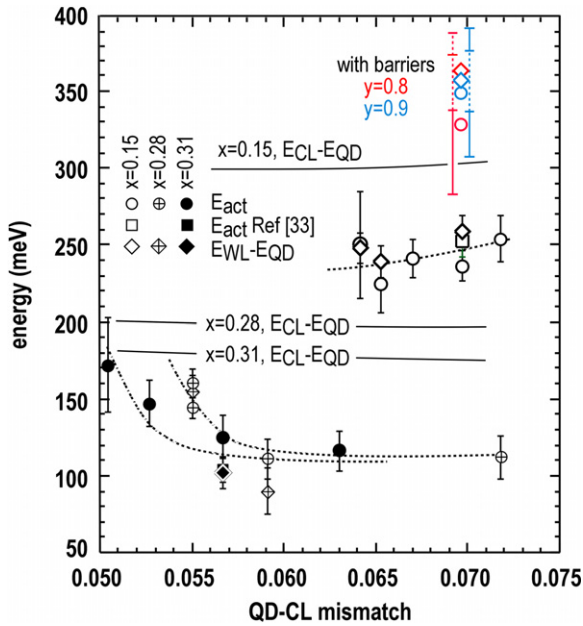


Figure 4. Difference ($E_{WL} - E_{QD}$, diamonds) of RT transition energies between confined states in WLs (E_{WL} , deduced by PR) and in QDs (E_{QD} , by PL) and PL activation energies (E_{act}) from [33] (squares) and this work (circles) as functions of the QD-CL mismatch for quantum dot strain-engineered structures with $x = 0.15, 0.28$ and 0.31 (open, crossed and full symbols, respectively). Black, red and blue symbols refer to structures without barriers and with $\text{In}_{1-y}\text{Al}_y\text{As}$ additional barriers with $y = 0.80$ and 0.90 , respectively. As for structures with barriers, continuous and dashed error bars are relative to E_{act} and ($E_{WL} - E_{QD}$) data points, respectively, while those on the left- and right-hand side of the symbols refer to $y = 0.8$ and 0.9 , respectively. Solid lines are model calculations [11] for the difference ($E_{CL} - E_{QD}$) of RT transition energies (E_{CL}) between CL states and E_{QD} . Dotted lines are guides for the eye.

the confined carriers' escape from QD levels, while E'_{act} may be related to extrinsic processes dependent on the presence of defects [11, 33].

In figure 4 the black symbols show the difference ($E_{WL} - E_{QD}$, diamonds) between WL (deduced by PR) and QD (by PL) transition energies at RT for structures without additional barriers; the mismatch was calculated from x and t following the procedure given in [11], whose validity was experimentally confirmed in [10, 34]. We plot $E_{WL} - E_{QD}$ as a function of the QD-CL mismatch since in QDSEd structures this parameter is one of the two parameters that determine the emission energy [11]; indeed the mismatch controls the strain exerted by CLs on QDs and, then, the energy gap of the QD material [11]. The other parameter is the band discontinuity between QDs and CLs that is determined by x [11].

In the same figure 4 we show the E_{act} activation energies obtained in this work (circles) and in [33] (squares) alongside model calculations [11] of the differences ($E_{CL} - E_{QD}$) between CL transition energy (E_{CL}) and E_{QD} (continuous lines). According to [19], under experimental conditions similar to ours, E_{act} is given by the sum of the activation energies for electron (E_{act}^e) and hole (E_{act}^h) escapes, shown in figure 1. From figure 4 we note that, when x is increased, the activation energies are significantly reduced. This has

an important effect on the temperature-dependent emission efficiency: under our experimental conditions when E_{act} is in the 250 meV range QDs emit also at RT, while for $E_{act} = 170$ meV and $E_{act} = 120$ meV PL emission is totally quenched at $T = 230$ K and $T = 150$ K, respectively. Moreover, figure 4 shows that, when $y = 0.90$ barriers are added to structures with a QD-CL mismatch of 0.0697 ($t = 60$ nm and $x = 0.15$), E_{act} increases from ~ 240 to ~ 350 meV and, correspondingly, the emission efficiency increases by a factor of 500, as shown in figure 3.

The activation energies are slightly dependent on the mismatch only for $x = 0.15$, while for $x = 0.28$ and 0.31 they increase when lattice mismatches are reduced to relatively small values due to increased strain relaxations. This effect could be related to the occurrence of cross-hatched InGaAs surfaces underneath QDs, whose roughness is well known to increase with larger strain relaxation of mismatched layers [35]; the roughness may likely affect WL thicknesses and, then, energies of WL-related confined states.

We note that, for all structures without barriers, E_{act} falls below ($E_{CL} - E_{QD}$), indicating the presence of an escape channel at an energy smaller than that of InGaAs CL states. We also note that, for all structures without barriers studied by both PL and PR, the activation energies coincide within the experimental error with ($E_{WL} - E_{QD}$), thus giving a strong indication that WL states are indeed the effective escape channels for carriers confined in QDs. Carriers reaching WLs may easily propagate along the quantum wells and, then, recombine on different types of non-radiative defects.

To further investigate the PL quenching process we consider now combined PR and PL studies on structures with $x = 0.15$ and $t = 60$ nm (corresponding to a QD-CL mismatch of 0.0697) where additional $\text{In}_{1-y}\text{Al}_y\text{As}$ barriers embedding QDs were added. In figure 4 we report the values of the difference ($E_{WL} - E_{QD}$, diamonds) between WL (deduced by PR) and QD (by PL) transition energies at RT for structures with barriers, alongside E_{act} activation energies (circles), using red and blue symbols for $y = 0.80$ and $y = 0.90$, respectively. Even if the error bars of activation energies are fairly large, we note that for these structures E_{act} is very close to ($E_{WL} - E_{QD}$), thus confirming the results of structures without barriers and strongly suggesting that WL states are indeed the effective escape channels for carriers confined in QDs.

In figure 5 we report the PL QD emission energy (E_{QD} , open circles), the PR WL transition energy (E_{WL} , full squares) and the sum ($E_{act} + E_{QD}$, full circles) of the activation energy E_{act} of PL quenching and E_{QD} as functions of y , which controls the additional barrier heights. The dotted lines represent the WL (E_{WL} , at ~ 1.220 eV) and the QD (E_{QD} , at ~ 0.950 eV) transition energies in structures without additional barriers, while the arrows show the effect of the insertion of barriers on E_{WL} and E_{QD} . The larger increase of E_{WL} as compared to that of E_{QD} can be interpreted as due to a larger extension of the carrier's wavefunction of WL states with respect to that of the QD ones that lie deeper in the potential wells. The extent of the E_{WL} and E_{QD} increments shows that the use of additional barriers has more favourable effects on the PL efficiency than deleterious ones related to the blueshifts

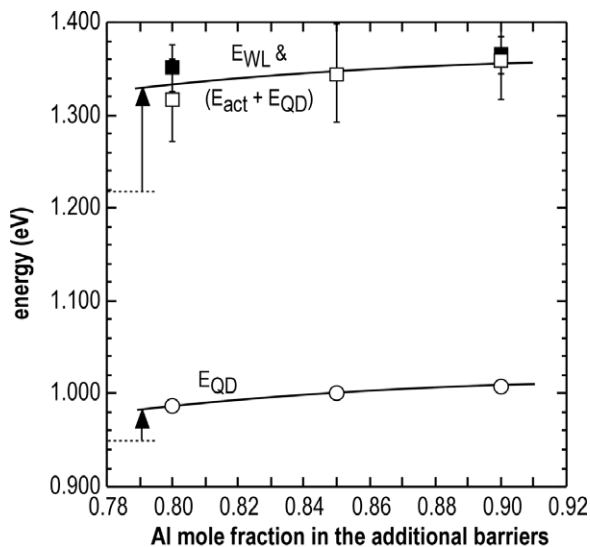


Figure 5. PL QD (E_{QD} , open circles), PR WL (E_{WL} , full squares) transition energies at RT along with the sum ($E_{act} + E_{QD}$) of E_{QD} and the activation energy E_{act} of PL thermal quenching (open squares) as functions of the Al composition of barriers y in quantum dot strain-engineered $\text{InAs}/\text{In}_x\text{Ga}_{1-x}\text{As}$ metamorphic structures ($x = 0.15$ and $t = 60$ nm) with $\text{In}_{1-y}\text{Al}_y\text{As}$ additional barriers. Dotted lines indicate values of E_{QD} and E_{WL} energies in structures with the same x and t , but without additional barriers. Vertical arrows show the effect of barriers on E_{QD} and E_{WL} . Solid lines are guides for the eye.

of transitions, which, at any rate, can be compensated for by small decreases of QD strain.

4. Conclusions

In conclusion, we have designed, grown by MBE and studied by photoluminescence and photoreflectance strain-engineered, metamorphic QD nanostructures on GaAs substrates with and without InAlAs enhanced barriers embedding InAs QDs. We were able to identify the relevant role of WL states in the carriers' escape process from QDs in both types of structures; our result points out that the energy separation between QD and WL states is an important factor in the design of QD nanostructures with efficient RT emission at long wavelengths. This conclusion is consistent with the observations that: (1) structures without additional barriers and with $x = 0.15$ emit at RT in the $1.3 \mu\text{m}$ range, while upon barrier insertion the emission is blueshifted by ~ 50 meV and (2) in structures without barriers the 10 K emission wavelength redshifts from 1.3 to $1.55 \mu\text{m}$ by increasing the CL composition from 0.15 to 0.35 , but the emission wavelength at RT does not exceed $1.44 \mu\text{m}$, owing to the PL thermal quenching [11]; on the other hand, structures with barriers do emit at RT at $1.39 \mu\text{m}$, $1.50 \mu\text{m}$ and $1.59 \mu\text{m}$ when $x = 0.35$, 0.40 and 0.45 , respectively [12].

The confident identification of the role of WLs suggests the possibility of different designs of structures to directly control WL states. Such approaches may include WL engineering and WL removal [36].

This could be an important result to extend RT emission of metamorphic QD structures to the $1.55 \mu\text{m}$ window and beyond, a topic of huge technological interest.

Acknowledgments

The work has been partially supported by the 'SANDiE' Network of Excellence of EC, contract no. NMP4-CT-2004-500101 and by the Italian Ministry of University and Research through FIRB contract RBAP06L4S5.

References

- [1] Bimberg D, Grundmann M and Ledentsov N N 1999 *Quantum Dot Heterostructures* (Chichester: Wiley)
- [2] Henini M 2008 *Handbook for Self-Assembled Semiconductor Nanostructures for Novel Devices in Photonics and Electronics* (Amsterdam: Elsevier)
- [3] Sargent E H 2005 *Adv. Mater.* **17** 515
- [4] Seravalli L, Frigeri P, Trevisi G and Franchi S 2008 *Appl. Phys. Lett.* **92** 213104
- [5] Liu H Y, Qiu Y, Lin C Y, Walther T and Cullis G 2008 *Appl. Phys. Lett.* **92** 111906
- [6] Mi Z, Bhattacharya P and Yang J 2006 *Appl. Phys. Lett.* **89** 153109
- [7] Ledentsov N N et al 2007 *J. Cryst. Growth* **301/302** 914
- [8] Seravalli L, Minelli M, Frigeri P, Allegri P, Avanzini V and Franchi S 2003 *Appl. Phys. Lett.* **82** 2341
- [9] Seravalli L, Minelli M, Frigeri P, Allegri P, Avanzini V and Franchi S 2005 *Appl. Phys. Lett.* **87** 063101
- [10] Geddo M, Guizzetti G, Patrini M, Ciabattini T, Seravalli L, Frigeri P and Franchi S 2005 *Appl. Phys. Lett.* **87** 263120
- [11] Seravalli L, Minelli M, Frigeri P, Franchi S, Guizzetti G, Patrini M, Ciabattini T and Geddo M 2007 *J. Appl. Phys.* **101** 024313
- [12] Seravalli L, Trevisi G, Minelli M, Frigeri P and Franchi S 2008 Engineering of quantum dot nano-structures for photonic devices *Handbook for Self-Assembled Semiconductor Nanostructures for Novel Devices in Photonics and Electronics* ed M Henini (Amsterdam: Elsevier) pp 505–28
- [13] Seravalli L, Minelli M, Frigeri P, Allegri P, Avanzini V and Franchi S 2007 *Mater. Sci. Eng. C* **27** 1046
- [14] Maximov M V et al 2000 *Phys. Rev. B* **62** 16671
- [15] Liu H Y, Sellers I R, Hopkinson M, Harrison C N, Mowbray D J and Skolnick M S 2003 *Appl. Phys. Lett.* **83** 3716
- [16] Chang K P, Yang S L, Chuu D S, Hsiao R S, Chen J F, Wei L, Wang J S and Chyi J Y 2005 *J. Appl. Phys.* **97** 083511
- [17] Seravalli L, Trevisi G, Frigeri P and Franchi S 2009 unpublished
- [18] Sanguinetti S, Henini M, Grassi Alessi M, Capizzi M, Frigeri P and Franchi S 1999 *Phys. Rev. B* **60** 8276
- [19] Le Ru E C, Fack J and Murray R 2003 *Phys. Rev. B* **67** 245318
- [20] Park Y M, Park Y J, Kim K M, Shin J C, Song J D, Lee J I and Yoo K H 2004 *Phys. Rev. B* **70** 035322
- [21] Torchynska T V, Casas Espinola J L, Borkovska L V, Ostapenko S, Dybiec M, Polupan O, Korsunskaya N O, Stintz A, Eliseev P G and Malloy K J 2007 *J. Appl. Phys.* **101** 024323
- [22] Nahory R E and Shay J L 1968 *Phys. Rev. Lett.* **21** 1569
Shay J L 1970 *Phys. Rev. B* **2** 803
- [23] Aspnes D E 1973 *Surf. Sci.* **37** 418
- [24] Pollak F H 1994 *Handbook on Semiconductors* vol 2, ed M Balkansky (Amsterdam: North-Holland) p 527

- [25] Briones F and Ruiz A 1991 *J. Cryst. Growth* **111** 194
- [26] Geddo M, Guizzetti G, Capizzi M, Polimeni A, Gollub D and Forchel A 2003 *Appl. Phys. Lett.* **83** 470
- [27] Shen H, Panad S H and Pollak F H 1988 *Phys. Rev. B* **37** 10919
Glembocki J and Shanabrook B 1992 *Semiconductors and Semimetals* vol 36, ed D G Seiler and C L Littler (Boston, MA: Academic) p 221
- [28] Aigouy L, Holden T, Pollak F H, Ledentsov N N, Ustinov W M, Kop'ev P S and Bimberg D 1997 *Appl. Phys. Lett.* **70** 3329
- [29] Rowland G L, Hosea T J C, Malik S, Childs D and Murray R 1998 *Appl. Phys. Lett.* **73** 3268
- [30] Poloczek P, Sek G, Misiewicz J, Loffler A, Reithmaier J P and Forchel A 2006 *J. Appl. Phys.* **100** 013503
- [31] Geddo M, Capizzi M, Patanè A and Martelli F 1998 *J. Appl. Phys.* **84** 3374
- [32] Rudno-Rudzinski W, Sek G, Ryczko K, Kudrawiec R, Misiewicz J, Somers A, Schwertberger A, Reithmaier J P and Forchel A 2005 *Appl. Phys. Lett.* **86** 101904
- [33] Mazzucato S, Nardin D, Capizzi M, Polimeni A, Frova A, Frigeri P, Seravalli L and Franchi S 2005 *Mater. Sci. Eng. C* **25** 830
- [34] Bellani V *et al* 2007 *Eur. Phys. J. B* **56** 217
- [35] Andrews A M, Speck J S, Romanov A E, Bobeth M and Pompe W 2002 *J. Appl. Phys.* **91** 1933
- [36] Mano T, Watanabe K, Tsukamoto S, Koguchi N, Fujioka H, Oshima M, Lee C D, Leem J Y, Lee H J and Noh S K 2000 *Appl. Phys. Lett.* **76** 3543